

Pairing states of superfluid ^3He in uniaxially anisotropic aerogel

Kazushi Aoyama and Ryusuke Ikeda

Department of Physics, Graduate School of Science, Kyoto University, Kyoto 606-8502, Japan

(Received 8 December 2005; published 16 February 2006)

Stable pairing states of superfluid ^3He in aerogel are examined in the case with a *global* uniaxial anisotropy which may be created by applying a uniaxial stress to the aerogel. Due to such a global anisotropy, the stability region of an Anderson-Brinkman-Morel (ABM) pairing state becomes wider. In a uniaxially stretched *aerogel*, the *pure* polar pairing state with a horizontal line node is predicted to occur, as a three-dimensional superfluid phase, over a measurable width just below the superfluid transition at $T_c(P)$. A possible relevance of the present results to the case with no global anisotropy is also discussed.

DOI: 10.1103/PhysRevB.73.060504

PACS number(s): 67.57.Bc, 67.57.Pq

In superconductivity and superfluidity, an intrinsic anisotropy has a profound effect on the resulting pairing state. For instance, one main origin of the $d_{x^2-y^2}$ pairing state in high- T_c cuprates¹ is the fourfold symmetry of the Fermi surface resulting from the crystalline anisotropy. Due to such an intrinsic and global anisotropy, a specific pairing symmetry with the highest temperature of Cooper instability is realized in the case of anisotropic superconductivity with no degeneracy between different pairing states. In contrast, the bulk liquid ^3He has an isotropic Fermi surface, and hence, there is a degeneracy in the transition point between different pairing states at least when the fluctuation is neglected.^{2,3} Recently, possible pairing states of superfluid ^3He in *globally isotropic* aerogels were examined by comparing the free energy in the Ginzburg-Landau (GL) region between different states, and it was found³ that, after averaging over the quenched disorder brought by the aerogel structure, the pairing states to be realized are unaffected by the *locally* anisotropic scattering events due to the aerogel. However, the situation may change if, as in the superconducting case mentioned above, a global anisotropy^{4,5} is introduced externally in the aerogel structure.

Here, we report on our results of theoretical phase diagrams of superfluid ^3He in an aerogel with *global* anisotropy. Throughout this paper, we assume that such an anisotropy may be induced in quasiparticle scattering events by applying a uniaxial stress^{4,5} to aerogels. Based on a conventional model⁶ of effects of aerogel on ^3He , the anisotropy can be incorporated in a momentum dependence of the *random-averaged* quasiparticle scattering amplitude. When the aerogel is uniaxially compressed, the two-dimensional (2D)-like pairing state is favored, and the region of the Anderson-Brinkman-Morel (ABM) pairing state becomes wider. In the stretched case, a 1D-like pairing state is favored at least near T_c , and actually the *pure* polar pairing state should be realized accompanied by a second order transition to a deformed ABM state at a lower temperature. This is a rare situation in which a new pairing state is expected to occur as a 3D superfluid phase of ^3He . This research was preliminarily reported elsewhere.⁷

Just as in Ref. 3, we start from the BCS Hamiltonian with an impurity potential term

$$\mathcal{H}_{\text{imp}} = \int d^3r \sum_{\sigma} \psi_{\sigma}^{\dagger}(\mathbf{r}) u(\mathbf{r}) \psi_{\sigma}(\mathbf{r}), \quad (1)$$

where $u(\mathbf{r})$ denotes an impurity potential for quasiparticles brought by aerogel structures. As argued in Ref. 3, the scattering amplitude $|u_{\mathbf{k}}|^2$ in an aerogel, where $u_{\mathbf{k}}$ is the Fourier transform of $u(\mathbf{r})$, should have a highly anisotropic and complicated momentum dependence, reflecting *local* anisotropy in aerogels. However, as far as the aerogel is globally isotropic, the local anisotropy is not reflected in averaged quantities such as $\overline{|u_{\mathbf{k}}|^2}$, where the overbar denotes the average over the impurity configuration due to the aerogel. On the other hand, in a globally anisotropic aerogel, $|u_{\mathbf{k}}|^2$ remains anisotropic. We invoke the model⁸

$$\overline{|u_{\mathbf{k}}|^2} = A[1 + \delta_u(\hat{\mathbf{k}} \cdot \hat{\mathbf{z}})^2], \quad (2)$$

where δ_u is a small parameter measuring the global anisotropy, $\hat{\mathbf{k}} = \mathbf{k}/k_F$, and $\hat{\mathbf{z}}$ denotes the direction of a uniaxial deformation. Although the factor A is a function of \mathbf{k}^2 , such an isotropic \mathbf{k} dependence induces no difference between various pairing states, and hereafter, A will be treated as a constant factor. Then, within the Born approximation, the quasiparticle Green's function $G_{\varepsilon}(\mathbf{p}) = (i\varepsilon - \xi_{\mathbf{p}} - \Sigma_{\mathbf{p}})^{-1}$ satisfies

$$\Sigma_{\mathbf{p}} = \int_{\mathbf{p}'} \frac{\overline{|u_{\mathbf{p}-\mathbf{p}'}|^2}}{i\varepsilon - \xi_{\mathbf{p}'} - \Sigma_{\mathbf{p}'}}}, \quad (3)$$

where ε is the fermionic Matsubara frequency, and $\int_{\mathbf{p}'} = \int d^3p'/(2\pi)^3$. Below, we will focus on the situations satisfying $2\pi\tau T \gg 1$, where $\tau^{-1} = 2\pi N(0) \langle \overline{|u_{\mathbf{k}}|^2} \rangle_{\hat{\mathbf{k}}}$ is the relaxation rate. Taking $\Sigma_{\mathbf{p}}$ to be purely imaginary and performing the \mathbf{p}' integral close to the Fermi surface, we obtain $\Sigma_{\mathbf{p}} = -i\eta_{\mathbf{p}} \text{sgn } \varepsilon$, where

$$\eta_{\mathbf{p}} = \frac{1}{2\tau} [1 + \tilde{\delta}_u(\hat{\mathbf{p}} \cdot \hat{\mathbf{z}})^2], \quad (4)$$

and $\tilde{\delta}_u = \delta_u(1 + \delta_u/3)^{-1}$. The neglect of the real part, $\text{Re}(\Sigma_{\mathbf{p}})$, of $\Sigma_{\mathbf{p}}$ is safely valid as far as $2\pi\tau T \gg 1$: The $\hat{\mathbf{p}}$ dependence in $\text{Re}(\Sigma_{\mathbf{p}})$ may be absorbed into an anisotropy of density of states (DOS), while such a correction to DOS is scaled by E_F^{-1} . Hence, the neglected correction to $\text{Re}(\Sigma)$ is of the order

$\delta_u/(E_F\tau)$, which is smaller than the magnitude of the particle-hole asymmetry T_c/E_F . In this manner, focusing on the imaginary part of Σ is justified. Then, $G_\varepsilon(\mathbf{p})$ becomes

$$G_\varepsilon(\mathbf{p}) = [i(|\varepsilon| + \eta_p)\text{sgn } \varepsilon - \xi_p]^{-1}. \quad (5)$$

Note that, when $\delta_u > 0$ (< 0), the mean free path of normal quasiparticles running along the z direction is shorter (longer). Thus, the case with $\delta_u > 0$ (< 0) corresponds to the uniaxially compressed (stretched) case.

Besides the self-energy part, the vertex part in the particle-particle channel is also affected by the impurity scattering. If neglecting spatial variations of the pair field $A_{\mu,i}$, the bare vertex \hat{p}_i is replaced by $\Gamma_i(\varepsilon, \mathbf{p})$, where

$$\Gamma_i(\varepsilon, \mathbf{p}) = \hat{p}_i + \int_{\mathbf{p}'} \Gamma_i(\varepsilon, \mathbf{p}') |G_\varepsilon(\mathbf{p}')|^2 |u_{\mathbf{p}-\mathbf{p}'}|^2. \quad (6)$$

The solution of Eq. (6) takes the form $\Gamma_i(\varepsilon, \mathbf{p}) = \hat{p}_i + (\hat{\mathbf{p}} \cdot \hat{\mathbf{z}}) \bar{\Gamma}_{\varepsilon, i}$, where

$$\bar{\Gamma}_\varepsilon = -1 + \left[1 - 2 \sum_{k \geq 1} \frac{1}{2k+1} \left(\frac{-\tilde{\delta}_u \tau^{-1}}{2|\varepsilon| + \tau^{-1}} \right)^k \right]^{-1}. \quad (7)$$

The above expressions will be used to derive a GL Hamiltonian per volume h_{GL} in the anisotropic case. Up to $O(\delta_u)$, its quadratic term is expressed by

$$\begin{aligned} h_{\text{GL}}^{(2)} &= A_{\mu,i}^* A_{\mu,j} \left[\frac{N(0)}{3} \left(\ln \frac{T}{T_{c0}} + T \sum_\varepsilon \frac{\pi}{|\varepsilon|} \right) \delta_{i,j} \right. \\ &\quad \left. - T \sum_\varepsilon \int_{\mathbf{p}} \hat{p}_i \Gamma_j(\varepsilon, \mathbf{p}) G_\varepsilon(\mathbf{p}) G_{-\varepsilon}(-\mathbf{p}) \right] \\ &\simeq \frac{N(0)}{3} \left[\ln \frac{T}{T_{c0}} + \psi \left(\frac{1}{2} + \frac{1}{4\pi T \tau} \right) - \psi \left(\frac{1}{2} \right) \right. \\ &\quad \left. + \frac{\delta_u}{4\pi T \tau} \psi^{(1)} \left(\frac{1}{2} + \frac{1}{4\pi T \tau} \right) \right] A_{\mu,i}^* A_{\mu,i} \\ &\quad + \frac{N(0)}{3} \frac{\delta_u}{4\pi T \tau} \frac{16}{15} \psi^{(1)} \left(\frac{1}{2} + \frac{1}{4\pi T \tau} \right) A_{\mu,z}^* A_{\mu,z}, \quad (8) \end{aligned}$$

where $\psi(z)$ is the di-gamma function, and $A_{\mu,i} \equiv |\Delta(T)| a_{\mu,i}$ with $a_{\mu,i} (a_{\mu,i})^* = 1$. The anisotropic term due to the vertex correction contributes to Eq. (8) with the same sign as that due to Σ_p .

The quartic term $h_{\text{GL}}^{(4)}$ is also derived in a similar manner and, up to $O(\delta_u)$, takes the form

$$\begin{aligned} h_{\text{GL}}^{(4)} &= \beta_1 |A_{\mu,i} A_{\mu,i}|^2 + \beta_2 (A_{\mu,i}^* A_{\mu,i})^2 + \beta_3 A_{\mu,i}^* A_{\nu,i}^* A_{\mu,j} A_{\nu,j} \\ &\quad + \beta_4 A_{\mu,i}^* A_{\nu,i}^* A_{\nu,j}^* A_{\mu,j} + \beta_5 A_{\mu,i}^* A_{\nu,i}^* A_{\nu,j}^* A_{\mu,j} \\ &\quad + [(\beta_1^{(1)} A_{\mu,i} A_{\mu,i} A_{\nu,z}^* A_{\nu,z} + \beta_2^{(1)} A_{\mu,i}^* A_{\mu,i} A_{\nu,z}^* A_{\nu,z} \\ &\quad + \beta_3^{(1)} A_{\mu,i} A_{\nu,i} A_{\mu,z}^* A_{\nu,z} + \beta_4^{(1)} A_{\mu,i}^* A_{\nu,i}^* A_{\nu,z}^* A_{\mu,z} \\ &\quad + \beta_5^{(1)} A_{\mu,i}^* A_{\nu,i}^* A_{\mu,z}^* A_{\nu,z}) + \text{c.c.}]. \quad (9) \end{aligned}$$

Each of the coefficients β_i is the sum of a weak coupling contribution $\beta_i^{(0)}$ and a strong coupling one $\delta\beta_i$. Regarding $\delta\beta_i$, their expressions with $\delta_u=0$ derived in Ref. 3 will be

used hereafter. This approximation should not affect calculation results except for extremely large $|\delta_u|$ values. The coefficients $\beta_i^{(0)}$ and $\beta_i^{(1)}$ are given by

$$\begin{aligned} \beta_3^{(0)} &= -2\beta_1^{(0)} = -\frac{\beta_0(T)}{7\zeta(3)} \left[\psi^{(2)} \left(\frac{1}{2} + \frac{1}{4\pi T \tau} \right) \right. \\ &\quad \left. + \frac{\delta_u}{4\pi T \tau} \psi^{(3)} \left(\frac{1}{2} + \frac{1}{4\pi T \tau} \right) \right], \end{aligned}$$

$$\begin{aligned} \beta_2^{(0)} &= \beta_4^{(0)} = -\beta_5^{(0)} = \beta_3^{(0)} - \frac{1}{4\pi T \tau} \frac{\beta_0(T)}{7\zeta(3)} \left[\left(\frac{5}{18} + \frac{\delta_u}{54} \right) \right. \\ &\quad \left. \times \psi^{(3)} \left(\frac{1}{2} + \frac{1}{4\pi T \tau} \right) + \frac{\delta_u}{4\pi T \tau} \frac{1}{18} \psi^{(4)} \left(\frac{1}{2} + \frac{1}{4\pi T \tau} \right) \right], \end{aligned}$$

$$\beta_3^{(1)} = -2\beta_1^{(1)} = -\frac{\delta_u}{4\pi T \tau} \frac{\beta_0(T)}{7\zeta(3)} \frac{46}{63} \psi^{(3)} \left(\frac{1}{2} + \frac{1}{4\pi T \tau} \right),$$

$$\begin{aligned} \beta_2^{(1)} &= \beta_4^{(1)} \\ &= -\beta_5^{(1)} = \beta_3^{(1)} - \frac{\delta_u}{4\pi T \tau} \frac{\beta_0(T)}{7\zeta(3)} \left[\frac{1}{9} \psi^{(3)} \left(\frac{1}{2} + \frac{1}{4\pi T \tau} \right) \right. \\ &\quad \left. + \frac{1}{4\pi T \tau} \frac{4}{27} \psi^{(4)} \left(\frac{1}{2} + \frac{1}{4\pi T \tau} \right) \right] \quad (10) \end{aligned}$$

up to $O(\delta_u)$, where $\beta_0(T) = 7\zeta(3)N(0)/(240\pi^2 T^2)$.

As seen in Eq. (8), the inclusion of a global anisotropy induces a splitting of the Cooper instability point between different pairing states. Since $\psi^{(1)}(y) > 0$ ($y > 0$), a uniaxial compression with positive δ_u makes the instability point of 2D-like pairing states with vanishing $a_{\mu,z}$ higher, implying that such a state must be realized just below $T_c(P)$. This situation is similar to ^3He thin films, and thus, this 2D-like state should be the ABM state. In the same manner, in the uniaxially stretched case with negative δ_u , the 1D-like polar pairing state with $a_{\mu,i} = \hat{d}_\mu \delta_{i,z}$ tends to occur just below T_c . However, it is unclear at this stage whether or not the state just below T_c may be a mixture of the ABM and polar pairing states⁹ so that the pure polar symmetry obtained at T_c crosses over upon cooling to the ABM one with no transition.

It should be noted that, in the disordered case, additional terms are induced in the GL Hamiltonian by the impurity scattering and its local anisotropy. When the global anisotropy is absent, a combination of one of the such terms and the gradient term, which was not represented in Eq. (8), leads to destruction of superfluid long-ranged order (LRO) in the ABM state.^{3,10} However, the contribution to the free energy of the additional term is well described simply by incorporating a disorder-induced shift of T_c into the *mean field* condensation energy E_c .³ In determining phase diagrams below, we have followed this finding³ and, for brevity, have used the disorder-induced T_c shift with $\delta_u=0$. The latter procedure does not affect our quantitative results unless *all* transitions between different pairing symmetries occur in the close vicinity of T_c .

We have numerically examined transitions between differ-

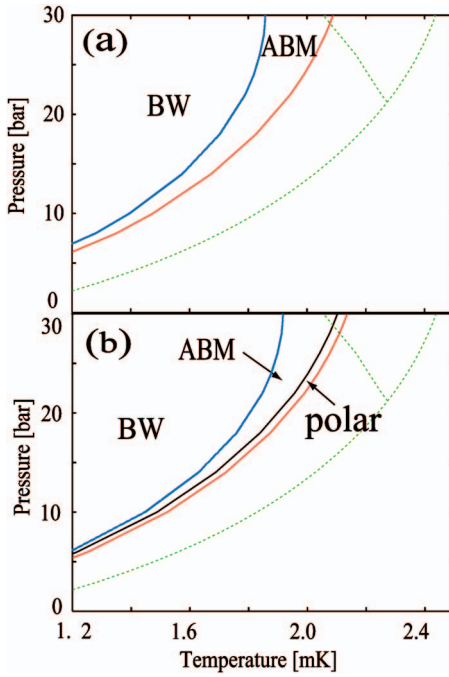


FIG. 1. (Color) Obtained P - T phase diagrams in a uniaxially compressed case (a) with $\delta_u = +0.04$ and a stretched case (b) with $\delta_u = -0.07$. For both figures, we have used $(2\pi\tau)^{-1} = 0.137(\text{mK})$. The solid curves are transition lines in aerogel, while the thin dotted curves are those of bulk liquid. The ABM state in (a) is a genuine superfluid with LRO, while in (b) it is a superfluid *glass* (Refs. 3 and 10).

ent pairing states through E_c by taking account of T_c shifts of different origins mentioned above. Since fully including 18 real components of the pair field $a_{\mu,i}$ is cumbersome, nonvanishing four components, $\text{Re } a_{\mu,\mu}$ and $\text{Im } a_{z,y}$, were kept in calculations so that the familiar ABM, Balian-Werthamer (BW), planar, and polar states are taken into account. For instance, in the uniaxially stretched case, the route through which only $\text{Re } a_{z,z}$ and $\text{Im } a_{z,y}$ remain nonzero is found to be the most favorable upon cooling from the Cooper instability of the polar state (see Fig. 2). Typical examples of the resulting phase diagrams for $\delta_u > 0$ (compressed case) and $\delta_u < 0$ (stretched case) are given in Figs. 1(a) and 1(b), respectively, where the GL Hamiltonian valid up to $O(\delta_u^2)$ was used. In both stretched and compressed cases, there is no polycritical pressure (PCP), i.e., there is a nonvanishing P range of the ABM state even in the low T limit. For the used τ value, there is no *mean field* stability region in $P < 30$ (bar) of the ABM state in the isotropic ($\delta_u = 0$) case. It implies that the main origin inducing the ABM state in the figures is the T_c shift and not the strong coupling effect. Further, we have verified that the planar pairing state cannot overcome the ABM one in free energy at any P and T and it is not realized as a pairing state in equilibrium.

In the ABM state in the compressed case, the direction of gap nodes is pinned on average along \hat{z} just like in thin films where the ABM or planar state has a wider stability region.⁴ An origin of the remarkably wide ABM region in Fig. 1(a) can be attributed to the similarity to the thin film case. Further, due to this pinning effect of \mathbf{l} -vector, this ABM state has

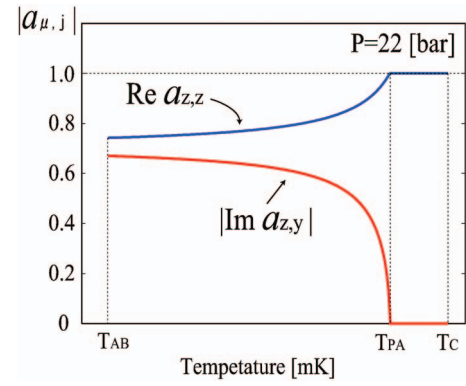


FIG. 2. (Color) Variation of $a_{\mu,i}$ at $P=22$ (bar) around the second order transition at T_{PA} between the polar and the deformed ABM states with $|\text{Re } a_{z,z}| \neq |\text{Im } a_{z,y}|$. The same material parameters were used as in 1(b). A first order transition to the deformed BW state occurs at T_{AB} .

a true superfluid LRO in contrast to the quasi-LRO in the isotropic case.³ On the other hand, in the stretched case (or equivalently, the case compressed in the cylindrically symmetric manner), the direction of gap nodes in the deformed ABM state (see Fig. 2) is *spontaneously* chosen within the x - y plane. This situation is similar to the bulk ^3He in a uniform magnetic field which also favors the ABM state. Thus, the ABM stability region becomes wider even in the stretched case, although this state is a superfluid *glass* with no genuine superfluid LRO.³ Further, in both cases, the BW state with no gap nodes is deformed by the anisotropy (i.e., $a_{x,x} = a_{y,y} \neq a_{z,z}$).¹¹

An intriguing result in the uniaxially stretched case is the appearance of the pure polar pairing state, with a horizontal line of gap nodes in the x - y plane, just below the $T_c(P)$ line. It appears that the temperature width over which the polar state is stable will be observable experimentally. Needless to say, this temperature width is, as well as that of the ABM state, extended with increasing $|\delta_u|$. This polar state is not a mixture with other pairing states and, as in Fig. 2, shows a second order transition to a deformed ABM state with point nodes in the x - y plane upon cooling. A T_c -shift dependent on the pairing states resulting from Eq. (8) is essential to obtaining the *pure* polar state. Since the direction $\hat{\mathbf{P}}$ of the gap maximum is pinned by \hat{z} , this polar state has a true superfluid LRO.

As a measure useful in detecting the polar state with the order parameter $A_{\mu,i} = \Delta \hat{d}_\mu \hat{P}_i$, a pulsed NMR frequency shift in the polar state will be considered. Here, $\hat{\mathbf{P}}$ points on averages to the stretched direction \hat{z} . Fluctuations of $\hat{\mathbf{P}}$ are assumed to be negligibly small. As usual, effects of the dipole energy on the spin dynamics can be examined in terms of Leggett's equations¹² as far as the initial configuration is in equilibrium. In the pure polar state, the so-called dipole torque \mathbf{R}_D^2 is given by

$$\mathbf{R}_D = -\frac{12g_D}{5}(\hat{\mathbf{d}} \cdot \hat{\mathbf{P}})(\hat{\mathbf{d}} \times \hat{\mathbf{P}}), \quad (11)$$

where g_D is a dipole energy strength,² and hence, $\hat{\mathbf{P}} \perp \hat{\mathbf{d}}$ and $\mathbf{H} \perp \hat{\mathbf{d}}$ are to be satisfied in equilibrium (see Fig. 3). Then, a

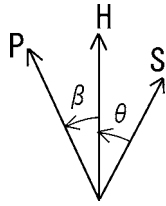


FIG. 3. Initial configuration to be taken in pulsed NMR experiments in the polar state. The angles θ and β are the tipping angles in $\mathbf{H}\text{-}\hat{\mathbf{P}}$ plane and $\cos^{-1}(\hat{\mathbf{P}}\cdot\mathbf{H}/H)$, respectively.

frequency shift $\Delta\omega$ of the free-induction signal due to \mathbf{R}_D occurring by tipping the magnetization by an angle θ is given by

$$\Delta\omega = \frac{\Omega_L^2}{2\omega} \left[(3 \cos^2 \beta - 1) \cos \theta + \frac{\sin^2 \beta}{2} (1 + \cos \theta) \right], \quad (12)$$

which depends on the angle β spanning $\hat{\mathbf{P}}$ and \mathbf{H} .

Finally, we note that the present result may also be relevant to liquid ^3He in globally *isotropic* aerogels³ if the correlation length ξ_a of the *local* anisotropy⁴ is much longer than the superfluid coherence length ξ_0 . Since, as mentioned earlier, the free energy of each pairing state is roughly determined by the condensation energy E_c even at length scales of the order of ξ_0 , the results induced by the global anisotropy,

such as the wider ABM region^{5,8} and an occurrence of the polar pairing state near T_c , may be valid in the globally isotropic aerogel under the condition $\xi_a \gg \xi_0$ which may be satisfied at higher pressures. Then, a polar *glass* phase with spatially random $\hat{\mathbf{P}}$ over long distances might be realized in the equal-spin pairing region near T_c . In contrast, at lower pressures with longer ξ_0 values, the anisotropy-induced T_c shift will be negligible, and the approach³ modeling the *local* anisotropy as a random field becomes appropriate. Then, a well-defined PCP is expected at a nonzero temperature.

In conclusion, by introducing a global anisotropy in aerogels, the region of the A-like phase should be extended if this phase has the ABM pairing state. A recent measurement has shown an extension of the A-like phase region, even on warming, due to a uniaxial compression.¹³ In aerogels deformed via a uniaxial stretch or a cylindrically symmetric compression, an appearance of the pure polar pairing state near T_c and a wider region of ABM superfluid glass³ are expected. We hope a measurement for the stretched case will be performed.

One of the authors (R.I.) is grateful to O. Ishikawa, Y. Lee, and J. A. Sauls for useful discussions. The present work was supported by the Grant-in-Aid for 21st Century COE ‘‘Center for Diversity and Universality in Physics’’ from the Ministry of Education, Culture, Sports, Science, and Technology (MEXT) of Japan.

¹For a review, see T. Timusk and B. Statt, Rep. Prog. Phys. **62**, 61 (1999).

²D. Volhardt and P. Wolfle, *The Superfluid Phases of Helium 3* (Taylor and Francis, London, 1990).

³K. Aoyama and R. Ikeda, Phys. Rev. B **72**, 012515 (2005).

⁴W. P. Halperin and J. A. Sauls, cond-mat/0408593 (unpublished).

⁵C. L. Vicente, H. C. Choi, J. S. Xia, W. P. Halperin, N. Mulders, and Y. Lee, Phys. Rev. B **72**, 094519 (2005).

⁶E. V. Thuneberg, S. K. Yip, M. Fogelstrom, and J. A. Sauls, Phys. Rev. Lett. **80**, 2861 (1998).

⁷R. Ikeda, presented in ULT2005 [<http://www.clas.ufl.edu/ULT2005/>].

⁸J. A. Sauls, presented in LT24 [<http://www.phys.ufl.edu/lt24/>], where a model similar to Eq. (2) was used to demonstrate an A-like phase region widened due to an anisotropy.

⁹Y. H. Li and T. L. Ho, Phys. Rev. B **38**, 2362 (1988).

¹⁰G. E. Volovik, JETP Lett. **63**, 301 (1996).

¹¹This deformed BW state is also expected to have no genuine LRO, because the ‘‘anisotropy’’ $a_{x,x}/a_{z,z}$ is T dependent and thus, does not become compatible with the anisotropy of the quenched disorder itself.

¹²A. J. Leggett, Rev. Mod. Phys. **47**, 331 (1975).

¹³W. P. Halperin, presented in ULT2005 (see Ref. 7).